Fundamental Study of Detection of Plastic Gear Failure Signs (Synchronization of a Non-Linear Oscillator with Mesh Frequency)

Daisuke Iba, J. Hongu, Hidetaka Hiramatsu, M. Nakamura, T. Iizuka, A. Masuda, I. Moriwaki and A. Sone

This paper proposes a new method — using neural oscillators — for filtering out background vibration noise in meshing plastic gear pairs in the detection of signs of gear failure. In this paper these unnecessary frequency components are eliminated with a feed-forward control system in which the neural oscillator's synchronization property works. Each neural oscillator is designed to tune the natural frequency to a particular one of the components.

Introduction

The trend towards an increase in plastic gear usage has continued because it is cost-effective; low-density; capable of absorbing vibration; its ability to operate with no lubrication, and so on. If the limitation of plastic gears relative to metal gears were to be improved as a result of new developments in both materials and processing, plastic gears could be used under more severe conditions, such as high load and/or high rotation speed. But even before that, if, say, an emergency shutdown system could be provided to respond in a safe manner, applications for plastic gears would be more widespread. And yet, there are not many studies concerning a failure detection system for plastic gears compared with metal gears.

Iba et al (Ref. 1) carried out rotation fatigue tests of POM (polyoxymethylene) gears using their developed power-absorb-type gear test rig, and analyzed effects of gear tooth cracks at their root on measured acceleration responses. The acceleration responses were measured with a pick-up set at the top of a housing of the driven-side gear shaft bearing during the operation tests; frequency analyses were carried out to identify dominant frequency components in the tests. As a result of the frequency analyses the responses included not only the DC, shaft frequency, its harmonics, fundamental meshing frequency, some mesh harmonics and its modulating sidebands, but also rolling elements noise of bearings, motor vibration and its harmonics, and so on. The particularly conspicuous frequency components in the responses were the shaft rotation frequency; fundamental meshing frequency; and some meshing harmonics and its modulating sidebands — whose frequency is the same as the shaft frequency. The responses were strongly affected by amplitude and frequency modulations. These modulation phenomena may be due to the fact that plastic gears are so flexible in that their tooth stiffness is lower than that of metal gears, and are thus subject to greater dimensional instabilities due to their larger coefficient of thermal expansion. These modulating components complicate the procedure of analysis of the acceleration responses and hide plastic-gear-failure signs. In the frequency analyses of the response data, the peak of the meshing frequency results in a slight change in complete tooth fracture. The response data include amplitude modulation; frequency modulation; rolling elements noise of bearings and motor; driving torque variation; and so on. Such complex data make detection of gear failure signs difficult, because the detection requires distinguishing slight changes in complex data.

On the other hand, non-linear oscillators — which were models for rhythm generators consisting of neurons — have been studied in biological study (Ref. 2) and are known as "neural oscillators." Neural oscillators have a specific property to synchronize with periodic, external inputs in a certain frequency range. Mathematical models of the neural oscillators were also proposed and examined (Refs. 3–4), and their applications to walking robots were reported (Refs. 5–6). Iba and Hongu studied a new control system for active, mass dampers using the mathematical model of the neural oscillators that can track the vibration behavior of high-rise buildings due to this synchronization characteristic (Refs. 7–8). These studies provide the knowledge that the neural oscillator can be used as an adaptive notch filter that filters out the background noise of vibration and follows a variation of a designated frequency — autonomously.

In this study a new signal processing method has been developed using neural oscillators to filter out the background noise of vibration in meshing plastic gear pairs for detection of failure signs. As mentioned above, the acceleration responses — which are measured at the top of the bearing housing during operating tests — include multiple frequencies. If these unnecessary frequency components were eliminated from the responses, it would be easy to detect gear failure signs. But the normal notch filter cannot follow the change in the designated, unnecessary frequencies by driving torque variation, and the adaptive notch filter needs a periodic reference signal to follow the change. Therefore a new filter system (or feed-forward-type noise-cancelling system) — using neural oscillators that can autonomously follow the change due to their synchronization properties — is developed in this study. Each neural oscillator is designed to tune the natural frequency to a particular frequency of the components. This tuning process is called on for the removal. Moreover, the output phase of the oscillators is set at a difference of 180° from the input phase, and is combined with

This paper was originally presented at the 2014 International Gear Conference, Lyon Villeurbanne, France and is republished here with the authors' permission.

the original, measured response to eliminate unnecessary components. The ultimate goal is to detect the failure signs of gears from the output of the proposed filter system, but while development of the filter system is discussed in this paper, there is no direct mention of its failure detection method. The basic concept of the proposed system is introduced, after which the neural oscillator that constructs the proposed filter system and the configuration of the feed forward control system are explained. Next, a simulated acceleration response of a meshing gear pair is constructed and the proposed noise cancellation system is applied to the simulated response to confirm the validity of the proposed system.

Neural Oscillator

In this section the mathematical model of a neural oscillator is introduced, and the synchronization property of the oscillator — a key capability of nonlinear oscillators — is explained.

Mathematical model. Here Matsuoka's neural oscillator is used as the neural oscillator (Refs. 3–4). The mathematical model of Matsuoka's neural oscillator is expressed as follows:

$$\dot{X}_{M,i}(t) = A_M X_{M,i}(t) + B_M \max(0, X_{M,i}(t)) + C_M = F_M(X_{M,i}(t)) \cdots i = 1,2 \tag{1}$$

Where, t is a time, and

$$X_{M,i}(t) = [x_{e,i}(t) \;\; x_{f,i}(t) \;\; x'_{e,i}(t) \;\; x'_{f,i}(t)]^{tr} \tag{2}$$

$$A_M = \begin{bmatrix} -1/\tau & 0 & -b/\tau & 0 \\ 0 & -1/\tau & 0 & -b/\tau \\ 0 & 0 & -1/T & 0 \\ 0 & 0 & 0 & -1/T \end{bmatrix}, B_M = \begin{bmatrix} 0 & -a/\tau & 0 & 0 \\ -a/\tau & 0 & 0 & 0 \\ 1/T & 0 & 0 & 0 \\ 0 & 1/T & 0 & 0 \end{bmatrix}, C_M = \begin{bmatrix} s/\tau \\ s/\tau \\ 0 \\ 0 \end{bmatrix} \tag{3}$$

This model contains two first-order lag elements to express excitation and inhibition, and can generate sustained oscillation. Generally, the five coefficients — s, τ, T, b, a — have been decided by identification of a biological neuron, but the specified animate being is not considered in this study. These parameters are chosen by our design method to generate the oscillation with a desired natural frequency (Ref. 8).

Further, in order to narrow the synchronization region to the rhythm generator, a mutual inhibition connection consisting of two neural oscillators is considered as follows:

$$\begin{cases} X_{M,1} = F_M(X_{M,1}) + G\max(0, X_{M,2}) \\ X_{M,2} = F_M(X_{M,2}) + G\max(0, X_{M,2}) \end{cases} \tag{4}$$

Where, considering the connection weight w, the matrix to connect the two oscillators is obtained as follows:

$$G = \begin{bmatrix} w & -w & 0 & 0 \\ -w & w & 0 & 0 \\ 0 & 0 & 0 & 0 \\ 0 & 0 & 0 & 0 \end{bmatrix} \tag{5}$$

Moreover, if $X_D = [X_{M,1} \;\; X_{M,2}]^{tr}$, the equation, which expresses the dynamics of the neural oscillator, is given as follows:

$$X_D = F_D(X_D) \tag{6}$$

Synchronization property. When the oscillator is subjected to an external periodic signal $p(\Omega t)$, the mathematical model of Matsuoka's neural oscillator becomes:

$$\dot{X}_D(t) = F_D(X_D) + E_D p(\Omega t) \tag{7}$$

Where, E_D is an input matrix as follows:

$$E_D = [\varepsilon \;\; -\varepsilon \;\; 0 \;\; 0 \;\; 0 \;\; 0 \;\; 0 \;\; 0]^{tr} \tag{8}$$

Here, ε is an input gain, and $p(\Omega t)$ is a normalized sinusoidal signal whose frequency is Ω. If the frequency Ω is partially close to the Eigen frequency ω_D of the neural oscillator, the oscillator is thus synchronized with the external sinusoidal wave.

This synchronization phenomenon can be seen when the detuning Ω-ω_D between the oscillator's frequency ω_D and the external periodic force's frequency Ω is a finite value. According to an analysis by the phase reduction method (Refs. 9–10), the synchronization region $\varepsilon\Gamma_{min} < \Omega - \omega_D < \varepsilon\Gamma_{max}$ is decided. Here, $\Gamma_{min,\,max}$ is the phase coupling function of the oscillator.

Figure 1 shows a synchronization region of the neural oscillator (Table 1). The colored area is the region also known as Arnold's tongue. In this figure the horizontal axis is the frequency Ω of input, and the vertical axis is the amplitude ε of input. It is clear that the synchronization region has spread from the oscillator's frequency $\omega_D = 1$ — when the amplitude of the external forcing is increased. The synchronization region depends on the amplitude of the forcing. Increased the coefficient for the external forcing in the neural oscillator, the region can be freely adjusted. The color in this figure shows the phase difference (phase locking points) between input/output of the neural oscillator.

Table 1 Parameters of neural oscillator

Parameters	Value
s	1.634
τ	0.212
T	2.54
b	2.52
a	2.52
w	-7.046

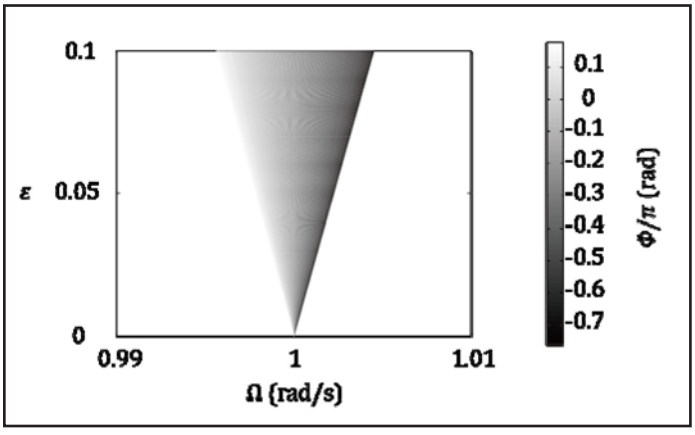

Figure 1 Synchronizing region of neural oscillator.

While the neural oscillator has a sensitive reaction to the sinusoidal input within the synchronization region, it does not have the same sensitivity to the input outside of the region. Thus the neural oscillator can be used as an adaptive, single-frequency generator, and as an adaptive notch filter to cancel the unnecessary frequency component in the vibration response of the meshing gears.

Gear Meshing

In this section a model of gear meshing vibration in a circumferential direction — used for verification of a proposed noise-can-

cellation system by simulation — is explained. Later, amplitude and frequency modulation caused by the eccentricities of gears are considered.

Dynamic loads on gear teeth. A simple vibration model in meshing gear pairs is used for simulation (Fig. 2). Each gear has a mass and is connected to the other by a spring and damper (Ref. 11). This vibration model — in a circumferential direction — is considered to be a single-degree-of-freedom vibration system as follows:

$$\ddot{x}_{th,\ meshing}(t) + 2\zeta_g \omega_g \dot{x}_{th,\ meshing}(t) + \omega_g^2 x_{th,\ meshing}(t) = \omega_g^2 e(t) \tag{9}$$

Where, $\ddot{x}_{th,\ meshing}(t)$ is spring deflection of the vibration system; ω_g is the natural frequency of the system; ζ_g is the damping ratio depending on the gear material; $e(t)$ is tooth profile

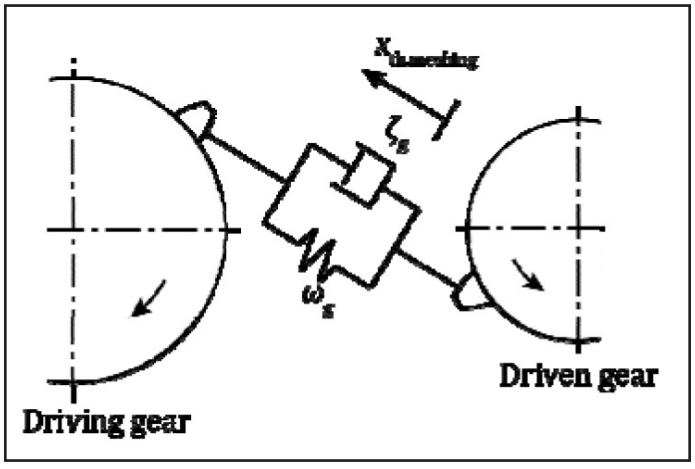

Figure 2 Vibration model in meshing gear pairs.

error — and this error is the input displacement to the system. Here it was assumed that the driving torque variation of the rotating shaft was small and the effect of the shaft stiffness on the line of action of force was small as well.

A meshing condition of a spur gear pair varies with time t. Considering the meshing period T_z, periodic change of total tooth stiffness during $0 \le t < z_2 T_z$ is expressed as follows:

$$T_{smooth}\dot{\omega}_g(t) + \omega_g(t) = \begin{cases} \sqrt{{\omega_{gj-1}}^2(t' + T_{1-2}) + {\omega_{gj}}^2(t')} & if\ 0 \le t' < T_{1-2} \\ \omega_{gj}(t') & else \end{cases} \tag{10}$$

In this study, the tooth profile error $e(t)$ is also expressed as follows:

$$e(t) = \begin{cases} E_0 \sin\left(\frac{\pi}{\varepsilon_{th} T_z}(t' + T_{2-1})\right) + E_0 \sin\left(\frac{\pi}{\varepsilon_{th} T_z} t'\right) \\ E_0 \sin\left(\frac{\pi}{\varepsilon_{th} T_z} t'\right) \end{cases} \tag{11}$$

Where, ε_{th} is contact ratio of the spur gear pair, and is obtained as follows:

$$t' = t - (j-1) \times T_z - r \times z_2 T_z \tag{12}$$

$\omega_{g,j}$ is the time-varying, natural frequency of the meshing gear system during meshing period that is derived from Ishikawa's tooth stiffness variation and the equivalent inertia mass on the pitch circle (Ref. 12). In addition, subscript j indicates the number of meshing tooth pairs, obtained as follows:

$$\begin{cases} j = fix\left(\frac{t - r z_2 T_z}{T_z}\right) + 1 \\ r = fix\left(\frac{t}{z_2 T_z}\right) \end{cases} \tag{13}$$

By using contact ratio ε_{th}, the transition time $T_{2\text{-}1}$ from two pair teeth in mesh to a single pair is obtained as follows:

$$T_{2-1} = (\varepsilon_{th} - 1) \times T_z \tag{14}$$

And T_{smooth} is a time constant of a first-order lag system to vary the natural frequency smoothly, here as $T_{smooth} = \sigma_{smooth} T_z$.

$X_{th,meshing}$ changes periodically, the timeframe dependent upon the rotation of the driven gear as follows:

$$x_{th,\ meshing}(t) = x_{th,\ meshing}(t + z_2 T_z) \tag{15}$$

Amplitude and frequency modulation by an eccentric error of a driven gear. Generally the vibration caused by the tooth-to-tooth meshing of a rotating gear pair contains various frequency components that are due not only to amplitude and frequency modulation caused by eccentricity of gears, but also to the rolling-elements noise of bearings, motor vibration and its harmonics, and so on. The effects of these unnecessary components on the measured vibration make detection of gear faults — such as gear tooth cracks — difficult.

In this subsection a model that includes the amplitude and frequency modulation caused by an eccentric error of a driven gear is considered. Considering the meshing frequency $\omega_z = 2\pi/T_z$, the periodic variable is expressed as follows:

$$x_{th,\ meshing}(\omega_z t) = x_{th,\ meshing}(\omega_z t + 2\pi) \tag{16}$$

The effect of amplitude and frequency modulation on the variable can be expressed as follows

(Ref. 13):

$$x_{th,\ meshing,\ AM,\ FM}(t) = \{1 + k_a \cos(\omega_m t)\} \times x_{th,\ meshing}\{\omega_z t + m_f \sin(\omega_m t)\} \tag{17}$$

Where,

$$\begin{cases} \omega_m = \omega_z / z_2 \\ m_f = e_2 \times \frac{z_2}{(1 + z_2/z_1)\sin\alpha} \end{cases} \tag{18}$$

and e_2 is the ratio of the radius of pitch circle of the driven gear to the eccentric error of the gear; k_a is the amplitude modulation factor; m_f is the frequency modulation factor; α is the pressure angle; and z the tooth number.

Numerical simulation of meshing gear vibration. According to the abovementioned gear model, numerical simulations of

Table 2 Parameters of gears

	Driving gear	Driven gear
Module (mm)	1.0	
Pres. angle (deg)	20.0	
Number of teeth	67	48
Face width (mm)	10	8
Equivalent inertia weight (kg)	1.8195	0.0085
Damping ratio	0.2	
Stiffness (GPa)	230	2.6
k_a	-	0.5
e_2	-	0.003
E_0 (mm)	0.001	
Revolution per second	-	50

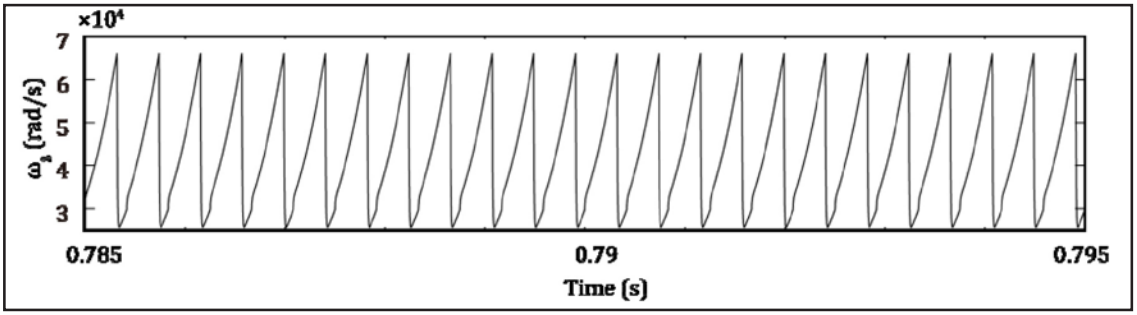

Figure 3 Natural frequency of gear meshing.

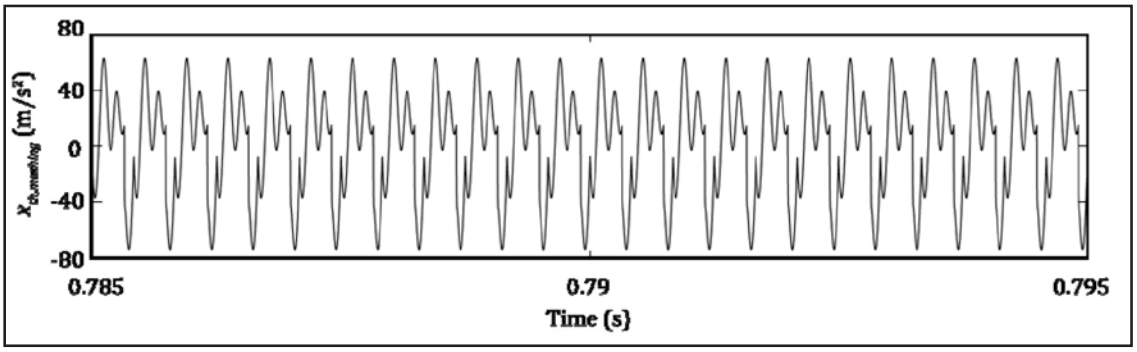

Figure 4 Acceleration response of gear meshing.

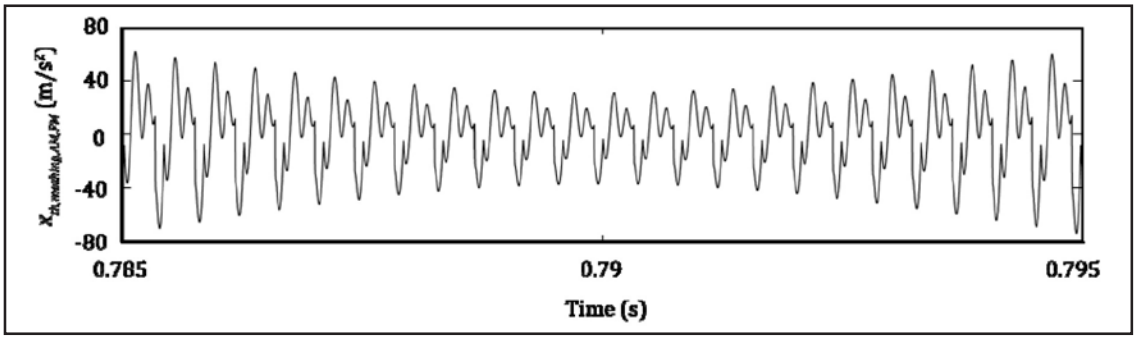

Figure 5 Acceleration response of gear meshing with AM and FM.

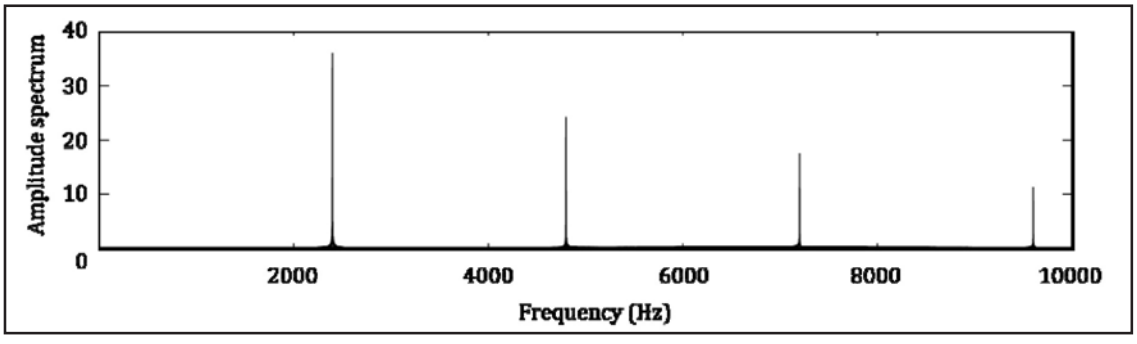

Figure 6 FFT of gear meshing.

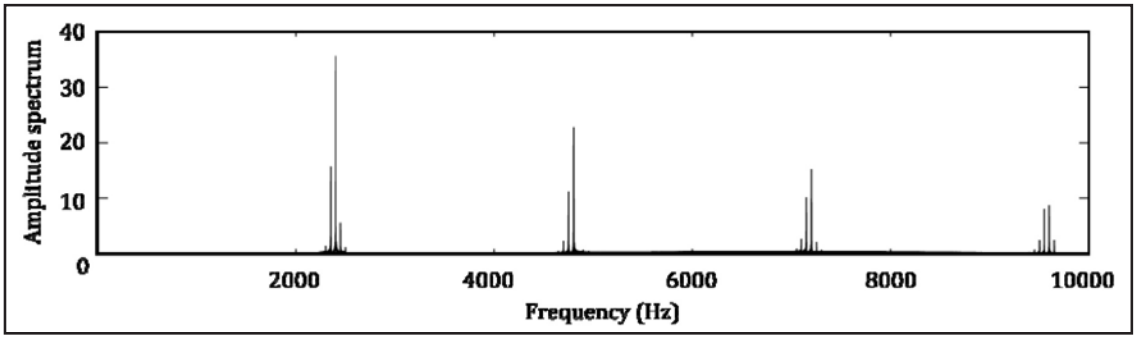

Figure 7 FFT of gear meshing with AM and FM.

meshing gears are carried out using the Runge-Kutta Fourth Order Method (Table 2). The step time of the simulations is $10^{-6}s$, and $\sigma_{smooth} = 10^{-2}$.

The results of numerical simulations are shown in following figures. Figure 3 shows the change of the natural frequency of the system. In this figure the natural frequency changed periodically because the meshing condition of a spur gear pair varied with time *t*. In considering the change of the natural frequency, the acceleration response of the system is obtained (Fig. 4). As for the eccentric error of the gear, the acceleration response of the system is subject to influence by both amplitude and frequency modulation (Fig. 5). Figures 6 and 7 show the frequency responses, with and without modulation, respectively. As a result of the modulation some sideband peaks can be seen (Fig. 7) when compared with Figure 6.

Noise-Canceling System

Here a noise cancellation system using neural oscillators to filter out the background noise of vibration in meshing plastic gear pairs for detection of failure signs of the gears is explained. The acceleration response, which is measured on the top of the housing at the gear shaft bearing, includes not only the DC; shaft frequency; its harmonics; fundamental meshing frequency; some mesh harmonics; and its modulating sidebands; but also rolling-elements noise of bearings, motor vibration and its harmonics, and so on. Detecting gear faults is much more difficult in the complex response; therefore these unnecessary frequency components should be eliminated from the response.

However, the frequency of the unnecessary components attracts a great amount of influence from the driving torque variation. The proposed new filter system using the neural oscillators can autonomously follow the frequency change of the unnecessary component due to the synchronization property (Fig. 8).

The proposed system has a measured signal and consists of some neural oscillators. The number of oscillators is the same as the number of unnecessary components. Each neural oscillator is designed to tune the natural frequency in to a particular frequency of the component. Moreover, the output of the oscillators is set to be out-of-phase with the input by 180° and is combined with the original, measured response to reduce the amplitude of the unnecessary components. The system is expressed as follows:

$$\begin{cases} X_{D,k} = F_{D,k}(X_{D,k}) + E_{D,k} s_g(t) \\ y(t) = s_g(t) - \sum_{k=1}^{n} \beta_{D,k} y_{D,k}(t - L_k) \end{cases} \quad (19)$$

where β_{Dk} is an arbitrary output gain of the oscillator, and L_k is a delay time of the system. Moreover, the output of the each oscillator is obtained as follows:

$$y_{D,k}(t) = [1 \ -1 \ 0 \ 0 \ 0 \ 0 \ 0 \ 0] \cdot \max(0, X_{D,k}) \quad (20)$$

Results of Numerical Simulation

In this section the proposed noise-cancellation system is applied to the simulated response to confirm validity of the system. In this simulation the analyzed signal consists of the abovementioned acceleration response and an unnecessary component 20sin (2π *7,250**t*), which is the same frequency of the modulated, third-order, high-frequency content.

Figure 9 shows the abovementioned acceleration response without the noise, and Figure 10 the signal with the noise; in both figures the time is multiplied by 2π *7,250.

As can be seen, the modulated noise complicates the acceleration response of gear meshing, even if the noise consists of the single component.

Next are shown the results of the noise cancellation system. The frequency of the neural oscillator was set to the frequency of the unnecessary component (Table 1). Figure 11 shows the output of the designed neural oscillator and the noise component; as can be seen, the output of the neural oscillator has the same frequency of the noise, and is out-of-phase by 180°.

Figure 12 shows the result of noise cancellation using the original output of the neural oscillator. In this simulation, $\varepsilon = 0.0002$ $\beta_D = 20/7$, $L = 5.5s$. In the figure the unnecessary component was reduced by the effect of the proposed filter, but discontinuous changes can be seen due to the non-linear property of the neural oscillator. This non-linear oscillator — having a sinusoidal input — has a limit cycle. If "phase" is pre-defined on the limit cycle, the phase and amplitude of the neural oscillator as a sinusoidal wave can be constructed by the defined "phase." To realize this construction, a phase map was used (Ref. 14). Figure 13 shows the result of noise cancellation using the constructed sinusoidal wave by the neural oscillator and the phase map. As can be seen, the original vibration of gear meshing is reconstructed.

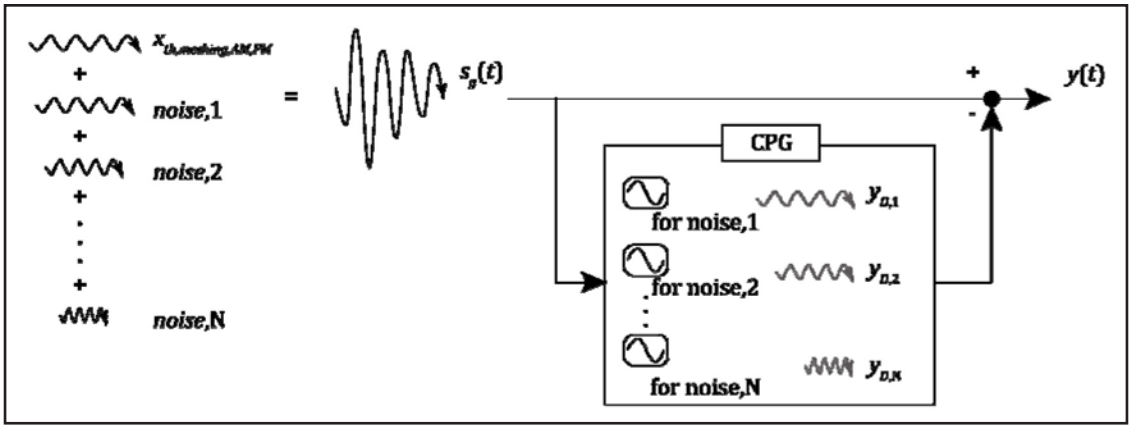

Figure 8 Concept of feed-forward noise cancelling system using neural oscillators.

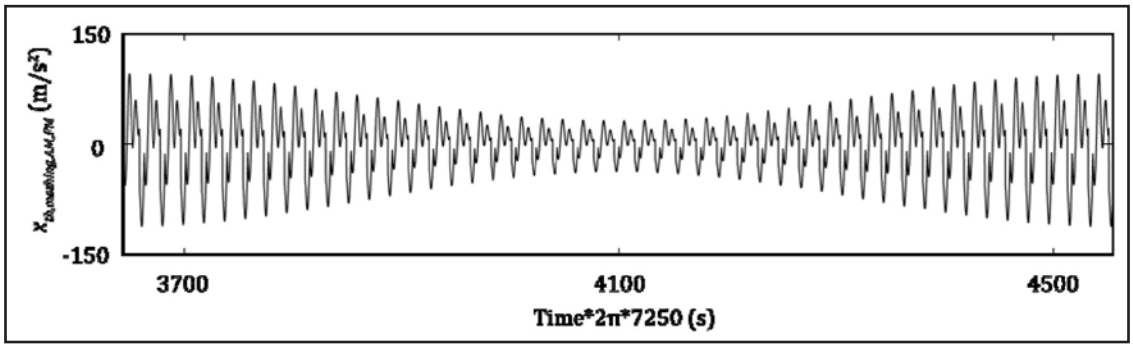

Figure 9 Acceleration response of gear meshing with AM and FM.

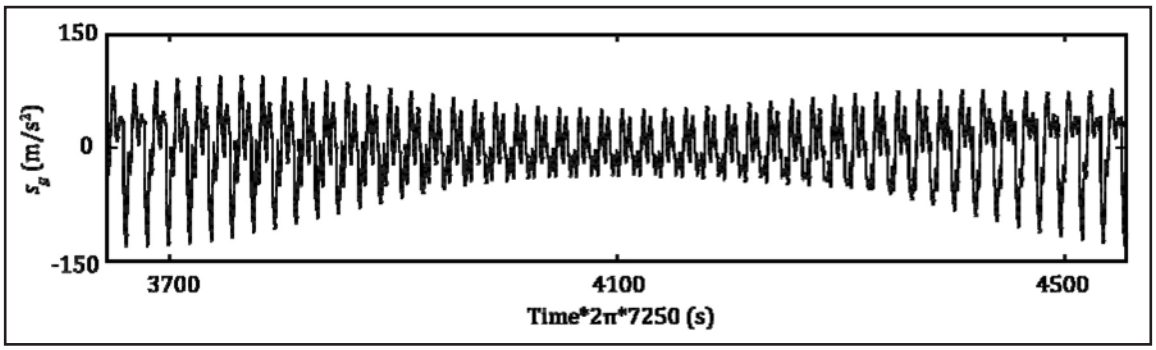

Figure 10 Acceleration response of gear meshing with AM, FM and external noise.

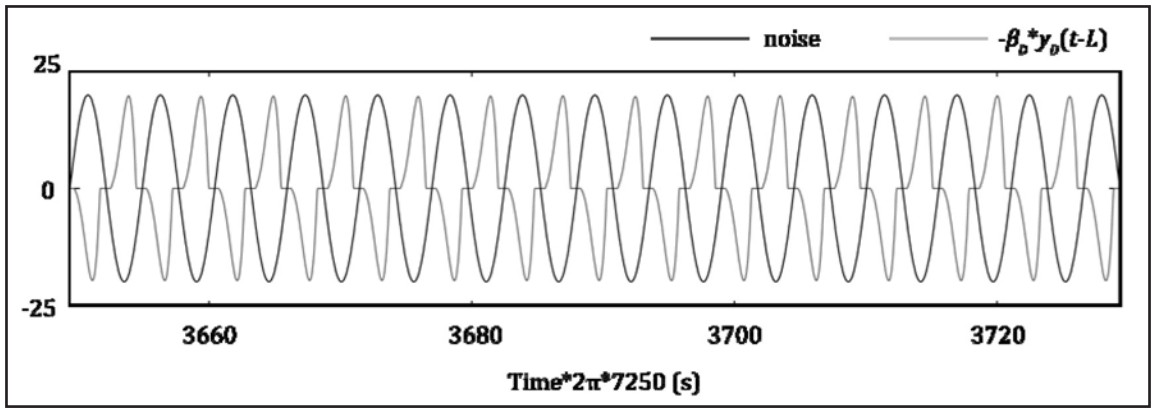

Figure 11 Output of the designed neural oscillator and noise component.

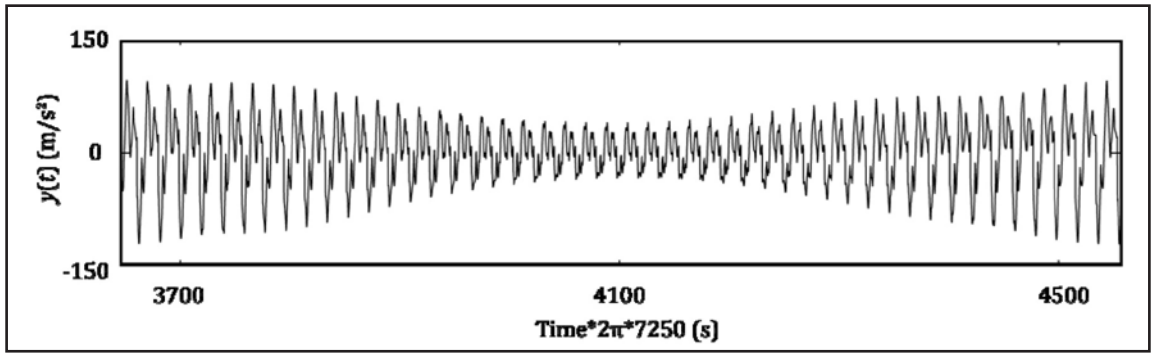

Figure 12 Result of noise cancellation using output of the neural oscillator.

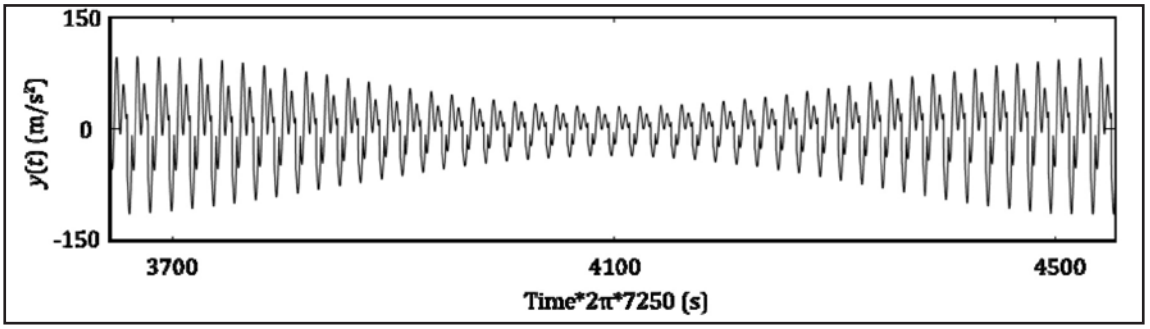

Figure 13 Result of noise cancellation using the constructed sinusoidal wave by the oscillator and phase map.

Conclusions

This paper proposed a new method using neural oscillators to filter out the background noise of vibration in meshing plastic gear pairs for detection of gear failure signs. It was shown how to eliminate unnecessary frequency components, with a feed-forward control system providing a neural oscillator's synchronization property. Each neural oscillator is designed to tune the natural frequency to a particular frequency of unnecessary components. The designed neural oscillators can follow the change in the driving torque variation autonomously, using their synchronization property. Moreover, the output of the oscillators is set to have a difference in the phase of 180 degrees from the input, and is included in the original measured response to reduce the amplitude of unnecessary components. The proposed noise cancellation method applied to the simulated response, and it was concluded that the proposed system could sufficiently eliminate unnecessary vibration content.

In future works we will design the suitable input and output gain for these oscillators, which could be determined through trial and error, and will confirm the oscillators' tracking properties. Furthermore, we will validate the multiple-elimination of unnecessary components and will apply the advanced system to the acceleration response measured by operating tests of gears, and assessing the efficacy of the system.

Acknowledgements. *The authors gratefully acknowledge the support of the department of mechanical and system engineering at the Kyoto Institute of Technology and Mitutoyo Association for Science and Technology, R1301.*

References

1. Iba, D., S. Ohmori, J. Hongu, M. Nakamura and I. Moriwaki. "Failure Detection of Plastic Gears Based on a Comparison of Fourier Coefficients of a Gear Mesh Vibration Model by Rectangle Pulse Train and Frequency Analysis of Acceleration Response," *2013 Trans. of the Japan Society of Mechanical Engineers Series C.* 79-808, 5138-5148, *http://dx.doi.org/10.1299/kikaic.79.5138.*
2. Shik, M. L. and G.N. Orlovsky. *Neurophysiology of Locomotor Automatism, Physiol.* Rev., 1976, 56, 465-501.
3. Matsuoka, K. "Sustained Oscillations Generated by Mutually Inhibiting Neurons with Adaptation," *Biological Cybernetics,* 1985, 52, 367-376.
4. Matsuoka, K. "Mechanisms of Frequency and Pattern Control in Neural Rhythm Generators," *Biological Cybernetics,* 1987, 56, 345-353.
5. Taga, G., Y. Yamaguchi and H. Shimizu. "Self-Organized Control of Bi-Pedal Locomotion by Neural Oscillators in Unpredictable Environment," *Biological Cybernetics*. 1991, 65, 147-159.
6. Fukuoka, Y. and H. Kimura. "Adaptive Dynamic Walking of a Quadruped Robot on Irregular Terrain based on Biological Concepts," 2003, *International Journal of Robotics Research,* 22-3-4, 187-202.
7. Iba, D. and J. Hongu. "Structural Vibration Control by Tuned Mass Damper Using Central Pattern Generator," 2011 *Proc. SPIE* 7981, *Sensors and Smart Structures Technologies for Civil, Mechanical, and Aerospace Systems,* 79814Q. DOI:10.1117/12.880406.
8. Hongu, J. and D. Iba. "Mutual Synchronization Between Structure and Central Pattern Generator," 2012 *Proc. SPIE 8345, Sensors and Smart Structures Technologies for Civil, Mechanical, and Aerospace Systems,* 83451E. DOI:10.1117/12.915045.
9. Kuramoto, Y. *Chemical Oscillations, Waves, and Turbulence*, 2003, Dover Press.
10. Pikovsky, A., M. Rosenblum and J. Kurths. *Synchronization: A Universal Concept in Non-Linear Sciences*, 2001, Cambridge University Press.
11. Umezawa, K., T. Sato and S. Ishikawa. "Simulation on Rotational Vibration of Spur Gears," *1983 Transactions of the Japan Society of Mechanical Engineers, Series C.* 49-441, 794-802 Series C.
12. Ishikawa, J. "On the Deflection of Gear Teeth," *1951 Transactions of the Japan Society of Mechanical Engineers,* 17-59, 103-106. http://dx.doi.org/10.1299/kikai1938.17.59_103.
13. Nishida, N. and Y. Maruki. "The Characteristic of Noise Spectrum of Gears with Eccentric Errors," *1981 Transaction of Japan Society of Precision Engineering,* 51 (3), 547-552.
14. Hongu, J., D. Iba, M. Nakamura and I. Moriwaki. "Vibration Control of Structures by a Dynamic Absorber Using a Neural Oscillator (Specification Method of Dynamic Absorber's Stroke Width Using an Amplitude Map), *The 56th Japan Joint Automatic Control Conference*, 2013, CD-ROM, No.129.

Hidetaka Hiramatsu is a student in Mechanical and System Engineering at Kyoto Institute of Technology, received his bachelor degree in mechanical engineering from Kyoto Institute of Technology in 2014. His research interest is gear failure detection by vibration analysis.

A PhD candidate student in design engineering at Kyoto Institute of Technology (KIT), **Junichi Hongu** began research in 2010 on application of neural oscillators for vibration control at KIT's Precision Manufacturing Laboratory. He subsequently in 2013 became a member of the project team researching gear failure by vibration analysis.

Daisuke Iba, associate professor of mechanical and system engineering at Kyoto Institute of Technology, received his Ph.D. degree in mechanical engineering from the institute in 2005, and his bachelor and master degrees in mechanical engineering from Hosei University in 1995 and 1997, respectively. Iba's research interests are structural response control and health monitoring, gear system condition monitoring and smart gear sensor development.

Arata Masuda, professor of mechanical engineering at Kyoto Institute of Technology, received his Ph.D degree in mechanical engineering there in 1999, and his BS from Kyoto University in 1990. His research has been in the area of smart structural systems and structural intelligence, including structural health monitoring, machine condition monitoring, vibration energy harvesting, vibration control and human motion monitoring and assistance.

Prof. Dr.Eng. Ichiro Moriwaki is a professor of mechanical and system engineering at Kyoto Institute of Technology and the director of the KIT Liaison Center. He received a doctorate degree of engineering from Kyoto University in 1989. He was the chairman of gearing committee in JSME in 2011-2013, and still a member of the committee. Moriwaki is also chairman of ISO / JIS standards committee in JGMA, a Japanese delegate for ISO TC 60.

Morimasa Nakamura has a Ph. D in engineering and is an assistant professor at the Kyoto Institute of Techonology. His primary research field is tribology, surface treatment technology and gearing.

Prof. Akira Sone earned his bachelor's, master's and Ph.D. degrees in mechanical engineering at Tokyo Metropolitan University in 1981, 1983 and 1987, respectively, working there as a research associate from 1987 to 1989. He has been on the faculty of the mechanical and system engineering department at Kyoto Institute of Technology since 1989. He has been an associate professor and a professor there since 1991 and 1999, respectively. Sone's research focus is seismic engineering and structural response control.